Deciphering the Role of Oncogenic MITFE318K in Senescence Delay and Melanoma Progression

Caroline Bonet, Flavie Luciani, Jean-François Ottavi, Justine Leclerc, Fanélie-Marie Jouenne, Marina Boncompagni, Karine Bille, Véronique Hofman, Guillaume Bossis, Gian Marco de Donatis, et al.

Oncogenic MITF^{E318K} promotes senescence delay and melanoma progression

Caroline Bonet[1,2,#], Flavie Luciani[3,4,#], Jean-François Ottavi[1,2,#], Justine Leclerc[1,2], Fanélie-Marie Jouenne[5], Marina Boncompagni[1,2], Karine Bille[1,2], Véronique Hofman[2,6], Guillaume Bossis[7], Gian Marco de Donatis[8], Thomas Strub[9], Yann Cheli[1,2], Mickaël Ohanna[1,2], Frédéric Luciano[10], Sandrine Marchetti[10], Stéphane Rocchi[1,2], Marie-Christine Birling[11], Marie-Françoise Avril[12], Nicolas Poulalhon[13], Thomas Luc[13], Paul Hofman[2,6], Jean-Philippe Lacour[14], Irwin Davidson[9], Brigitte Bressac-de Paillerets[5,15, #], Robert Ballotti[1,2,#], Jean-Christophe Marine[3,4,#], and Corine Bertolotto[1,2,*]

1, INSERM, U1065 (équipe 1), Equipe labélisée ARC 2016, C3M, 06204, Nice, France

2, University of Nice Sophia-Antipolis, UFR Médecine, 06204, Nice, France

3, Center for Human Genetics, KU Leuven, 3000 Leuven, Belgium

4, Center for the biology of disease, VIB, 3000 Leuven, Belgium

5, Service de Génétique, Institut de Cancérologie Gustave Roussy, Villejuif, France

6, Inserm, ERI21/EA 4319, Nice, F-06107, France

7, CNRS-UMR 5535, Montpellier, F-34293, France

8, INSERM, U1065 (équipe 12), C3M, 06204, Nice, France

9, Institut de Génétique et de Biologie Moléculaire et Cellulaire, CNRS, INSERM, Université de Strasbourg, Illkirch, France

10, INSERM, U1065 (équipe 2), C3M, 06204, Nice, France

11, Institut Clinique de la Souris–Mouse Clinical Institute, Illkirch, France

12, AP-HP, Hôpital Cochin -Tarnier, Service de Dermatologie et Faculté Paris Descartes, 75006, Paris, France

13, Centre Hospitalier Universitaire de, Department of Dermatology, 69495, Lyon, France

14, Centre Hospitalier Universitaire de Nice, Service de Dermatologie, 06204, Nice, France

15, INSERM U1186, Immunologie intégrative des tumeurs et génétique oncologique, Paris, France

# These authors equally contributed to this work.

* Correspondence should be addressed to Corine Bertolotto: bertolot@unice.fr

The authors disclose no potential conflicts of interest.

Abstract

BACKGROUND*: MITF* encodes an oncogenic lineage-specific transcription factor in which a germline mutation (*MITF^{E318K}*) was identified in human patients predisposed to both nevus formation and, among other tumor types, melanoma.

METHODS: Here, we used a newly generated Mitf^{E318K} knock-in (KI) mouse model and human melanocytes, from MITF^{E318K} patients, to determine the role of the mutation in vivo and to characterize the mechanisms underlying the oncogenic activity of MITF^{E318K}.

RESULTS: Using proximity ligation assay, we demonstrate a decrease in endogenous MITF SUMOylation, in melanocytes from patients with MITF^{E318K} (mean of cells with hypoSumoylated MITF, MITF^{E318K} vs MITF^{WT}, 94 vs 44 %, difference= 50, 95% CI 21.8 to 67.2, p=0.0039). The Mitf^{E318K} mice are slightly hypopigmented (mean melanin relative content Mitf^{WT} vs Mitf$^{E318K/+}$, 1 vs 0.67, difference=-0.33, 95% CI= -0.5 to -0.07, p= 0.0191) and we provide genetic evidence that Mitf^{E318K} enhances BRaf^{V600E}-induced nevus formation in vivo (mean nevus number for Mitf^{E318K}; BRaf^{V600E} vs Mitf^{WT}; BRaf^{V600E} 44 vs 68, difference=24, 95% CI= 9.1 to 38.9, p= 0.0059). Importantly, although Mitf^{E318K} is not sufficient to cooperate with BRaf^{V600E} alone in promoting metastatic melanoma, it accelerates tumor formation on a BRaf^{V600E}; Pten-deficient background (median survival for Mitf^{E318K} vs Mitf^{WT} 42 vs 51 days, ratio=0.8, 95% CI of ratio= 0.3 to 2.0, p=0.0009). Transcriptome analysis suggests a decrease in senescence in tumors from MITF^{E318K} mice. We confirmed this hypothesis, by in vitro experiments, demonstrating that Mitf^{E318K} impairs the ability of human melanocytes to undergo BRAF^{V600E}-induced senescence.

CONCLUSION: We characterized the functions of melanoma-associated MITF^{E318K} mutations. Our results demonstrate that MITF^{E318K} reduces the program of senescence to potentially favor melanoma progression in vivo.

Microphthalmia-associated transcription factor (MITF) is a key transcription factor that plays a pivotal role in melanocytes and melanoma development. MITF is also involved in the implementation of the resistance to targeted- or immuno-therapy [1, 2]. Although the role of MITF was a matter of debate a few years ago, it appears now that melanoma cells are able to switch from a low-MITF to a high-MITF phenotype, thereby adapting to micro-environmental conditions such as hypoxia, inflammation or drug treatments [3-5]. MITF is part of a transcriptional program implemented by melanoma cells to switch from an invasive/mesenchymal status to a differentiated/fast-growing phenotype [6]. MITF silencing was also demonstrated to inhibit melanoma cell proliferation and to induce senescence [7, 8].

A few years ago, a germline variant of *MITF* (p.E318K) was reported to predispose carriers to melanoma and kidney cancer [9, 10]. Using in vitro assays, we and others demonstrated that this mutation impairs MITF SUMOylation and affects the transcriptional activity of MITF. However, the mechanisms by which MITF^{E318K} contributes to melanoma progression remain uncharacterized.

Senescence, a state of stable cell cycle arrest, is a tumor suppressor mechanism that is activated in response to oncogenic events (oncogene-induced senescence, OIS). One of the best examples of senescence *in vivo* is human nevus, a benign proliferation of cutaneous melanocytes and an early step in melanoma progression. Nevi frequently express oncogenic BRAF^{V600E} and can remain growth arrested for decades due to OIS [11, 12], demonstrating that senescence provides an efficient suppression of cell proliferation. Primary melanoma can be viewed as a paradigm of senescence evasion, and the bypass of BRAF^{V600E}-induced senescence triggers melanoma progression [13, 14].

Here, we demonstrated that melanocytes isolated from patients harboring MITF^{E318K} display a decreased endogenous MITF SUMOylation status compared with healthy melanocytes. We also generated a new knock-in (KI) mouse model that expresses endogenous

Mitf^{E318K}. Although Mitf^{E318K} was not sufficient to trigger melanoma, it increased BRAF^{V600E}-induced nevus formation. Moreover, *Mitf*^{E318K} accelerated melanoma progression in a BRaf^{V600E} and Pten-deficient background. Transcriptomic analysis of tumors indicates that *Mitf*^{E318K} favored proliferation and altered the expression of key senescence players such as CDKN2B and CDKN2A, suggesting that Mitf^{E318K} might favor OIS evasion. In cultured melanocytes, we demonstrated that hypo-SUMOylated MITF (MITF^{E318K}) delays BRAF^{V600E}-induced OIS and its associated growth arrest. Collectively, our data provide new mechanistic insights underlying the oncogenic role of the naturally occurring mutant of MITF, namely MITF^{E318K}, and demonstrate that MITF^{E318K} exerts its pro-melanoma effect by favoring senescence bypass.

Methods summary

Melanocytes were obtained from skin biopsies and were collected with participants' informed signed consent. Cells were transduced with an empty or BRAF^{V600E} lentiviral particles. Interactions between MITF and SUMO were detected by in situ proximity ligation assay (Sigma). *Mitf*$^{E318K/+}$ knock-in (KI) animals were generated at the Mouse Clinical Institute in Illkirch, France (http://www-mci.u-strasbg.fr). Animal experiments were performed at the Animal Facilities of the C3M institute and the KU Leuven under the conditions established by the European Community (Directive 86/609/CCE) and according to French and Belgian laws. Gene expression arrays were performed by the Nice-Sophia Antipolis Genomics Platform. Mean values of ratios and Benjamini-Hochberg adjusted p-values are shown. Senescence β-galactosidase staining was assessed according to manufacturer's protocol (Ozyme). All statistical tests were two-sided. We used the *t* test to calculate 95% CIs on differences between means and to obtain the *P* value (GraphPad Prism).

Full Methods and any associated references are available in the supplementary section.

Results

Study of endogenous MITF^{E318K} SUMOylation in patients' melanocytes.

The MITF missense substitution p.E318K occurs in a consensus SUMOylation site. Furthermore, after over-expression of MITF and SUMO, we and others demonstrated that the mutation reduces MITF SUMOylation [9, 10]. However, these artifact conditions do not confirm that endogenous MITF SUMOylation is indeed affected. To remove this doubt, we used a proximity ligation assay (PLA) with anti-MITF and anti-SUMO antibodies. Experiments in melanocytes isolated from patient harboring the MITF^{E318K} mutation revealed a dramatic decrease in the number of dots compared with melanocytes isolated from the skin of healthy donors, reflecting MITF hypo-SUMOylation in MITF^{E318K} melanocytes (Figure 1A). Quantification of dots in 3 cultures of normal human melanocytes (NHM) and 4 cultures of MITF^{E318K} melanocytes demonstrated a significant increase in the number of cells exhibiting a low level of MITF SUMOylation in the MITF^{E318K} melanocytes (mean 0-1 dot, green background for MITF^{E318K} vs MITF^{WT} 94 vs 44 %, difference= 50, 95% CI 21.8 to 67.2, p=0.0039), whereas the number of NHM displaying between 2 to 4 or 5 to 9 dots was markedly increased compared to MITF^{E318K} melanocytes (Figure 1B). Collectively, these results indicate a global loss of MITF SUMOylation in the MITF^{E318K} melanocytes. Appropriate controls, including the use of anacardic acid, a SUMOylation inhibitor, or cells in which wild-type or mutant MITF^{E318K} was expressed, validated our approach (supplemental Figures 1A-E).

Role of Mitf^{E318K} in melanoma development in vivo

To establish the role of MITF^{E318K} in melanoma occurrence *in vivo*, we generated a new knock-in (KI) mouse model that expresses Mitf^{E318K} from its endogenous promoter (supplemental Figures 2A-G). Noteworthy, heterozygous and homozygous *Mitf^{E318K}* mice are

slightly hypopigmented, resulting in a subtle reduction in the color of the coat, ear, tail and paws compared with control littermates. Fontana-Masson silver stain and melanin quantitation confirmed that the level of melanization was decreased in ear and tail tissues from Mitf$^{E318K/+}$ mice compared with control littermates (mean melanin relative content Mitf^{WT} vs Mitf$^{E318K/+}$ 1 vs 0.67, difference=-0.33, 95% CI= -0.5 to -0.07, p= 0.0191) (Figures 2 A-B and supplemental Figure 3).

The *Mitf^{E318K}* mutant mice also did not exhibit signs of nevi or melanoma development within 24 months of birth. Next, we generated Mitf$^{E318K/+}$ mice in a Tyr::CreER$^{T2/°}$; BRaf$^{CA/+}$ background and analyzed melanoma development following topical application of 4-hydroxy-tamoxifen on the back skin of adult mice. Compared with *Mitf* wild-type control littermates, a significant increase in the number of nevi was observed in Mitf$^{E318K/+}$; BRaf$^{V600E/+}$ mice (mean nevus number for Mitf^{E318K}; BRaf^{V600E} vs Mitf^{WT}; BRaf^{V600E} 44 vs 68, difference=24, 95% CI= 9.1 to 38.9, p= 0.0059) (Figure 2C and supplemental Figure 4A). Kaplan-Meier analysis revealed no significant difference in the survival between Mitf$^{E318K/+}$ and wild-type Mitf mice (Supplemental Figure 4B). In this mouse model, Mitf^{E318K} did not decrease the median latency of melanoma development nor its penetrance. Tumors from both groups were all predominantly amelanotic and histologically comparable. The tumor cells displayed a spindle-morphology and were only locally invasive (supplemental Figure 4C).

Then, we investigated whether Mitf^{E318K} might facilitate melanomagenesis on the BRaf$^{V600E/+}$; Pten-deficient background. After topical application of 4-hydroxy-tamoxifen on the back skin of adult mice Mitf$^{E318K/+}$; Tyr::CreER$^{T2/°}$; BRaf$^{CA/+}$; Pten$^{f/f}$ mice, melanoma development was analyzed. Pigmented lesions developed earlier and more rapidly in the Mitf$^{E318K/+}$; BRaf$^{V600E/+}$; Pten$^{-/-}$ mice compared with BRaf$^{V600E/+}$; Pten$^{-/-}$ control littermates (Figure 2D). Tumors from both groups exhibited comparable histological features with a spindle morphology as described above (supplemental Figure 4D). Importantly, Mitf$^{E318K/+}$;

BRaf$^{V600E/+}$; Pten$^{-/-}$ mice displayed a decreased survival time compared with BRaf$^{V600E/+}$; Pten$^{-/-}$ mice (median survival for Mitf^{E318K} vs Mitf^{WT} 42 vs 51 days, ratio=0.8, 95% CI of ratio= 0.3 to 2.0, p=0.0009) (Figure 2E).

These data indicate that Mitf^{E318K} favors melanoma progression on the BRaf$^{V600E/+}$; Pten$^{-/-}$ background.

To better understand the mechanisms by which Mitf^{E318K} favors melanoma development, we profiled the transcriptomes of Mitf wild-type and Mitf^{E318K} tumors. Statistical analysis showed that 300 genes were differentially expressed between Mitf$^{E318K/+}$; BRaf$^{V600E/+}$; Pten$^{-/-}$ and BRaf$^{V600E/+}$; Pten$^{-/-}$ tumors. In total, 131 genes were upregulated and 169 were downregulated. The list of top fifty up- and down-regulated genes is presented in Supplemental Table 1. Among the top activated biological functions associated with the genes differentially expressed, Ingenuity Pathway Analysis identified “Hematological System development” (p-value range from 2.2E-3 to 1E-5) and the annotations included “quantity of blood cells,” "quantity of leukocytes" and “quantity of B lymphocytes" with a Z score between 1.66 and 2.48 (supplemental Table 2). Indeed, *Cd79a* and *Cd79b*, which are known B cell markers, were among the most upregulated genes (supplemental Table 1), and 10 out of 14 regulated genes fitted with an increase in B lymphocyte infiltration (supplemental Figure 5). Our findings suggested an increase in B-cell infiltration in the Mitf$^{E318K/+}$; BRaf$^{V600E/+}$; Pten$^{-/-}$ tumors that might favor tumor progression in these mice.

Ingenuity Pathway Analysis also identified “G1 phase” (Z-score= -1,958, p-value=1E-3) and “senescence of tumor cells” (Z-score= -1,6, p-value=1E-3) as top biological functions inhibited in Mitf$^{E318K/+}$; BRaf$^{V600E/+}$; Pten$^{-/-}$ tumors compared with BRaf$^{V600E/+}$; Pten$^{-/-}$ tumors. Within the “senescence of tumor cells” pathway, the expression of 5 out of 6 genes in Mitf$^{E318K/+}$; BRaf$^{V600E/+}$; Pten$^{-/-}$ tumors are consistent with an inhibition of senescence (Figure

2F). Among them, the cyclin-dependent kinase inhibitors Cdkn2a (encoding both p16/Ink4A and p19Arf) and Cdkn2b play key roles in melanocyte senescence [15].

These observations suggest that MITF^{E318K} might exert its pro-melanoma effect through an inhibition of oncogene-induced senescence.

Effect of MITF^{WT} and MITF^{E318K} in BRAF^{V600E}-induced senescence

To test this hypothesis, we used immortalized Mel-ST melanocytes as a model system. These cells express undetectable levels of MITF [16], thus allowing direct comparison of phenotypes induced by exogenous wild-type and mutant without interference with endogenously expressed MITF. After transduction, Mel-ST melanocytes expressed comparable levels of wild-type or mutant MITF^{E318K} (Figure 3A). As expected, forced BRAF^{V600E} expression induced a robust stimulation of ERK phosphorylation in all conditions (Figure 3A). BRAF^{V600E} stimulated SA-β-gal activity that was barely affected by forced expression of MITF^{WT}, while forced expression of MITF^{E318K} almost completely prevented the induction of SA-β-gal activity (Figure 3B). BRAF^{V600E} also decreased bromodeoxyuridine (BrdU) incorporation in control (EV+EV vs EV+BRAF^{V600E}, 40 vs 13%, difference=-27, 95% CI -33.1 to -20.3, p=0.0009) and to a lesser extent in MITF^{WT} cells (Mi^{WT}+EV vs Mi^{WT}+BRAF^{V600E}, 40 vs 25%, difference=-15, 95% CI -26.8 to -4.6, p=0.0204), whereas BRAF^{V600E} did not affect BrdU incorporation in cells with forced expression of MITF^{E318K} (Figure 3C). MITF^{E318K} efficiently prevented the increase in SA-β-gal activity (Figure 3B) and the decrease in BrdU incorporation (Figure 3C) caused by BRAF^{V600E}. Importantly, the level of both cell cycle inhibitors p21 and p16 was reduced in MITF^{E318K} compared with wild-type MITF-expressing cells (Figure 3A). Consistent with these observations, expression of MITF^{E318K} but not MITF impaired BRAF^{V600E}-increased cell size and granularity, two additional senescence parameters (supplemental Figures 6A-B).

Using melanocytes isolated from skin of healthy donors or patients with the MITF^{E318K} mutation, we confirmed that MITF^{E318K} impaired oncogene-induced senescence. Indeed, forced expression of BRAF^{V600E} in both wild-type MITF and MITF^{E318K} melanocytes promoted activation of ERK (Figure 3D). BRAF^{V600E} induced SA-βGal staining in two different wild-type MITF melanocyte cultures (HM1-Mi^{WT} + EV vs HM1-Mi^{WT} + BRAF^{V600E} 10 vs 46%, difference=36, 95% CI= 15.1 to 56.7, p=0.0087 and HM2-Mi^{WT} + EV vs HM2-Mi^{WT} + BRAF^{V600E} 8 vs 65%, difference= 57, 95% CI=22.2 to 91.0, p= 0.0102) but not in two different MITF^{E318K} melanocyte cultures (Figures 3E-F). However, MITF^{E318K} melanocytes do undergo senescence upon forced expression of BRAF^{V600E} when cultured for a longer period time (not shown). It should be noted that MITF^{E318K} melanocyte cultures display a decreased doubling time compared with MITF^{WT} melanocytes (57 hours versus 67 hours) (supplemental Figure 6C).

One may wonder why MITF^{E318K} can exert its anti-senescence effect in Mel-ST and human melanocytes, which are not supposed to have a constitutive activation of the PI3K pathway, in contrast to the mouse model. However, when assessing AKT activation in Mel-ST and in human melanocytes in our culture medium, we observed a basal phosphorylation of AKT, indicating an activation of the PI3K pathway (supplemental Figures 6D-E). Therefore, in cultured cells, MITF^{E318K} might also cooperate with PI3K to prevent senescence. In conclusion, these findings demonstrate that the naturally occurring MITF^{E318K} mutant severely impairs oncogene-induced senescence.

Discussion

SUMOylation is difficult to investigate given the dynamic and labile nature of this process. Forced expression of both the SUMO machinery and the target has been widely used to efficiently detect the SUMO-modified proteins, yet it may generate some unspecific SUMO

conjugation. Detecting endogenous SUMOylation remains a challenge. Here, using PLA, we demonstrated for the first time the endogenous hypo-SUMOylated status of MITF^{E318K}.

To establish the link between the MITF^{E318K} melanoma-susceptibility genes and pathogenesis mechanisms, we also constructed a new mouse model harboring the endogenous MITF^{E318K} point mutation. In this model, we observed pigmentation lightening. Additionally, upon BRaf$^{V600E/+}$ expression, our results reveal an increase in nevus count. Both observations were consistent with the phenotypes described in MITF^{E318K} heterozygous patients [10, 17]. These data suggest that melanocytes expressing both BRAF^{V600E} and MITF^{E318K} can proliferate longer before entering senescence. This finding is reminiscence of patients with biallelic inactivation of the cell cycle inhibitor CDKN2A, which results in enhanced cell proliferation, who display an increased number of nevi [18]. The decrease in pigmentation might be ascribed to impairment of the differentiation process.

Mitf^{E318K} affects melanoma development in the BRAF$^{V600E/+}$;Pten$^{-/-}$ mice background but not in a BRAF^{V600E} only background. This finding suggests that MITF^{E318K} should cooperate with the PI3K pathway to overcome senescence.

Activation of the PI3K pathway was thought to fully overcome BRAF^{V600E}-induced senescence [14, 19]. However, stabilized β-catenin, which can act as an anti-senescence effect, accelerates melanoma progression in BRAF$^{V600E/+}$;Pten$^{-/-}$ mice [20, 21]. MITF^{E318K}, which accelerates melanoma progression in BRAF$^{V600E/+}$;Pten$^{-/-}$ mice, might also exert an anti-senescence effect in vivo.

Transcriptome analysis of wild-type or Mitf$^{E318K/+}$ tumors in the BRaf$^{V600E/+}$;Pten$^{-/-}$ background suggests that Mitf^{E318K} might prevent senescence and favor cell proliferation. This hypothesis has been confirmed in cultured cells as we demonstrated that Mitf^{E318K} inhibits BRaf^{V600E}-induced senescence. This observation appears at odds with mice results indicating that MITF^{E318K} requires PI3K activation to exert its pro-melanoma effect. However,

in cultured cells, despite the absence of an activating mutation in the PI3K pathway, we observed a basal activation of AKT that might strengthen the anti-senescence effect of MITF^{E138K}.

Among the genes differentially regulated in these tumors, none are MITF or MITF^{E318K} targets. Noteworthy, transcriptomic analysis in cultured melanoma cells did not allow us to identify specific MITF^{E318K} targets (unpublished data); however, we and others have demonstrated an increase in the transcriptional activity of MITF^{E318K} [9, 10]. Thus, we were unable to find the appropriate window to identify the MITF^{E318K} targets or MITF^{E318K} might induce a weak effect on a large set of genes that cannot pass the statistical threshold. This is not surprising given that MITF^{E138K} is not strongly oncogenic but rather a medium penetrance susceptibility allele. Furthermore, this finding is consistent with our ChIP-seq experiments demonstrating that MITF^{E318K} is redistributed over the genome on a larger repertoire of low affinity genomic sequence compared to wild-type MITF [9].

SUMOylation could induce a conformational change of MITF and impact the MITF interaction with its partner proteins. In addition, SUMO creates specific interactions with proteins containing SUMO-interacting motifs (SIMs) through a non-covalent bound. Therefore, the MITF^{E318K} mutation will severely impair theses interactions. Interestingly, the related family members TFE3 and TFEB [22, 23] are among the known MITF interactors. This interaction with MITF might be affected by the E318K mutation. Although the functional roles of MITF-TFE heterodimers in melanoma remain to be elucidated, it should be noted that TFE3 and TFEB are involved in kidney cancer [24], the incidence of which is also increased in carriers of the MITF^{E318K} mutation. Additionally, MITF interacts with the chromatin remodeler BRG1 [22, 25]; thus, MITF could impact chromatin organization and global transcriptional regulation. Again, the MITF^{E318K} mutation and the resulting SUMOylation alteration might affect the MITF interaction with BRG1, leading to the

modification of the MITF target gene repertoire. This hypothesis is strengthened by the identification of a potential SUMO-interacting motif in BRG1 (GPS-SUMO, http://sumosp.biocuckoo.org/). However, only a small proportion of the available proteins typically needs to be SUMOylated to achieve a biological effect [26]. Because of this process, referred to as the "SUMO enigma," it has not been possible to identify such SUMO-dependent MITF interactors to date.

In conclusion, genetic-association studies have been widely used in the search for cancer-susceptibility genetic variants, but few studies have established the link between these variants and the pathogenesis mechanisms. This approach should allow important insights into the pathways of tumor development and might ultimately lead to more effective individually targeted cancer-prevention strategies. Here, we characterized the alterations of MITF functions caused by the p.E318K mutation. Our results demonstrate that MITF^{E318K} impaired the implementation of the senescence program and thus potentially favors melanoma progression.

Acknowledgements

The authors would like to thank H. Arnheiter (NIH, Bethesda, USA), Lionel Larue and Véronique Delmas (Institut Curie, Paris) for their helpful comments on experiments involving mouse models and James Wordsworth for his assistance in proximity ligation assay. We acknowledge the support of the Nice-Sophia Antipolis Genomics Platform for microarray analysis. The authors would also like to thank the C3M and VIB animal facilities. The Mel-ST melanocytes were kindly provided by Dr. Robert Weinberg (Whitehead Institute, USA). This work was funded by la Société Française de Dermatologie, Melanoma Research Alliance (MRA Team Science Award #269626), ANR-13-BSV1-0025-01 to R.B., Fondation pour la Recherche Médicale, La Ville de Nice, Cancéropôle PACA to C.B, INCa grant 2013-1-MELA-05 to B.B-d.P. Grant Fondation Gustave Roussy 2009, n°PRI-2010-18 to B.B-d.P., Grant 2011 ITMO-Plan Cancer to B.B-d.P, ICGC n°201102 to B.B-d.P.

Author Contributions

C Bertolotto, JCM, BB-DP, RB, ID designed, analyzed and wrote the manuscript. GB, FL and SR participated in the scientific discussions. MCB contributed to the creation of the mouse model. MFA, NP, TL, PH, JPL and SM collected biological samples. C Bonet, FL, JL, JFO, FMJ, MB, KB, VH, GMDD, TS, and YC performed the functional analysis.

References

1. Johannessen CM, Johnson LA, Piccioni F, *et al.* A melanocyte lineage program confers resistance to MAP kinase pathway inhibition. Nature 2013;504(7478):138-42.

2. Muller J, Krijgsman O, Tsoi J, *et al.* Low MITF/AXL ratio predicts early resistance to multiple targeted drugs in melanoma. Nat Commun 2014;5:5712.

3. Cheli Y, Giuliano S, Fenouille N, *et al.* Hypoxia and MITF control metastatic behaviour in mouse and human melanoma cells. Oncogene 2012;31(19):2461-70.

4. Ohanna M, Cheli Y, Bonet C, *et al.* Secretome from senescent melanoma engages the STAT3 pathway to favor reprogramming of naive melanoma towards a tumor-initiating cell phenotype. Oncotarget 2013;4(12):2212-24.

5. Ohanna M, Giuliano S, Bonet C, *et al.* Senescent cells develop a PARP-1 and nuclear factor-{kappa}B-associated secretome (PNAS). Genes Dev 2011;25(12):1245-61.

6. Hoek KS, Goding CR. Cancer stem cells versus phenotype-switching in melanoma. Pigment Cell Melanoma Res 2010;23(6):746-59.

7. Giuliano S, Cheli Y, Ohanna M, *et al.* Microphthalmia-associated transcription factor controls the DNA damage response and a lineage-specific senescence program in melanomas. Cancer Res 2010;70(9):3813-22.

8. Strub T, Giuliano S, Ye T, *et al.* Essential role of microphthalmia transcription factor for DNA replication, mitosis and genomic stability in melanoma. Oncogene 2011;30(20):2319-32.

9. Bertolotto C, Lesueur F, Giuliano S, *et al.* A SUMOylation-defective MITF germline mutation predisposes to melanoma and renal carcinoma. Nature 2011;480(7375):94-8.

10. Yokoyama S, Woods SL, Boyle GM, *et al.* A novel recurrent mutation in MITF predisposes to familial and sporadic melanoma. Nature 2011;480(7375):99-103.

11. Davies H, Bignell GR, Cox C, *et al.* Mutations of the BRAF gene in human cancer. Nature 2002;417(6892):949-54.

12. Michaloglou C, Vredeveld LC, Soengas MS, *et al.* BRAFE600-associated senescence-like cell cycle arrest of human naevi. Nature 2005;436(7051):720-4.

13. Kuilman T, Michaloglou C, Vredeveld LC, *et al.* Oncogene-induced senescence relayed by an interleukin-dependent inflammatory network. Cell 2008;133(6):1019-31.

14. Vredeveld LC, Possik PA, Smit MA, *et al.* Abrogation of BRAFV600E-induced senescence by PI3K pathway activation contributes to melanomagenesis. Genes Dev 2012;26(10):1055-69.

15. McNeal AS, Liu K, Nakhate V, *et al.* CDKN2B Loss Promotes Progression from Benign Melanocytic Nevus to Melanoma. Cancer Discov 2015;5(10):1072-85.

16. Gupta PB, Kuperwasser C, Brunet JP, *et al.* The melanocyte differentiation program predisposes to metastasis after neoplastic transformation. Nat Genet 2005;37(10):1047-54.

17. Sturm RA, Fox C, McClenahan P, *et al.* Phenotypic Characterization of Nevus and Tumor Patterns in MITF E318K Mutation Carrier Melanoma Patients. J Invest Dermatol 2013; 10.1038/jid.2013.272.

18. Sviderskaya EV, Gray-Schopfer VC, Hill SP, *et al.* p16/cyclin-dependent kinase inhibitor 2A deficiency in human melanocyte senescence, apoptosis, and immortalization: possible implications for melanoma progression. J Natl Cancer Inst 2003;95(10):723-32.

19. Dankort D, Curley DP, Cartlidge RA, *et al.* Braf(V600E) cooperates with Pten loss to induce metastatic melanoma. Nat Genet 2009;41(5):544-52.

20. Damsky WE, Curley DP, Santhanakrishnan M, *et al.* beta-catenin signaling controls metastasis in Braf-activated Pten-deficient melanomas. Cancer Cell 2011;20(6):741-54.

21. Delmas V, Beermann F, Martinozzi S, *et al.* Beta-catenin induces immortalization of melanocytes by suppressing p16INK4a expression and cooperates with N-Ras in melanoma development. Genes Dev 2007;21(22):2923-35.

22. Laurette P, Strub T, Koludrovic D, *et al.* Transcription factor MITF and remodeller BRG1 define chromatin organisation at regulatory elements in melanoma cells. Elife 2015;4.

23. Pogenberg V, Ogmundsdottir MH, Bergsteinsdottir K, *et al.* Restricted leucine zipper dimerization and specificity of DNA recognition of the melanocyte master regulator MITF. Genes Dev 2012;26(23):2647-58.

24. Bressac de-Paillerets B, Lesueur F, Bertolotto C. A germline oncogenic MITF mutation and tumor susceptibility. Eur J Cell Biol 2013; 10.1016/j.ejcb.2013.10.002.

25. Mehta G, Kumarasamy S, Wu J, *et al.* MITF interacts with the SWI/SNF subunit, BRG1, to promote GATA4 expression in cardiac hypertrophy. J Mol Cell Cardiol 2015;88:101-10.

26. Wilkinson KA, Henley JM. Mechanisms, regulation and consequences of protein SUMOylation. Biochem J 2010;428(2):133-45.

Figure Legends

Figure 1. Endogenous MITF^{E318K} exhibits a hypo-SUMOylated status. (A) MITF-SUMO interactions detected by PLA in normal human melanocytes isolated from the skin of three different MITF wild-type donors (HM-Mi^{WT}) or from four different patients carrying the MITF^{E318K} mutation (HM-Mi^{E318K}). **(B)** Automatic quantification of the image data from 100 cells per patient was performed with the BlobFinder software. The graph presents the number of 0-1 dots; 2-4 dots or 5-9 dots /nuclei (abscissa) and frequency of cells (ordinates) with

dots/nuclei. The green box highlights the increase proportion of MITF-^{E318K} cells with 0-1 dots/nuclei compared with MITF-^{WT} cells.

Figure 2. Mitf^{E318K} induces pigmentation lightening, increases nevus number in cooperation with BRaf$^{V600E/+}$ and enhances melanomagenesis in the BRaf$^{V600E/+}$/Pten$^{-/-}$ background. (A) H&E and Fontana-Masson staining of tail sections of 10-month-old mice with the indicated genotypes. Magnification 200x. **(B)** Melanin content determined from skin ear of 10-month-old mice with the indicated genotypes. Results are expressed as relative melanin content compared to MitfWT mice. Experiments were performed in triplicate. **(C)** The number of nevi was determined by counting three different areas (representing almost the whole back) of mice (n=5) aged between 25 and 29 days after 4-hydroxy-tamoxifen (4-OHT) application **(D)** Tumor phenotype after localized application of 4-OHT at the adult stage. Representative time-lapse photographs are presented. **(E)** Kaplan-Meier survival plot of Mitf^{E318K} (n=12) or wild-type Mitf (n=8) littermates after localized induction in the BRaf$^{V600E/+}$; Pten$^{-/-}$ background. p value (log-rank *Mantel–Cox test)* is indicated. **(F)** Circular network showing the genes differentially regulated between Mitf^{WT} and Mitf^{E381K} and associated with senescence. The regulation of five out of six genes is consistent with an inhibition of "senescence in tumor cells" (blue dotted lines). The genes upregulated in Mitf^{E318K} tumors are noted in red, and genes that are downregulated are noted in green. The yellow line indicates that the finding underlying the relationship is inconsistent with the state of the downstream node based on existing literature data.

Figure 3. MITF^{E318K} impairs oncogene-induced senescence in melanocyte cells. (A) Mel-ST melanocytes were transduced with control (EV) or BRAF^{V600E} lentiviral particles and an empty adenovirus (EV) or adenoviruses encoding either myc-tagged MITF wild-type (Mi^{WT})

or myc-tagged MITF^{E318K} for three weeks and were subjected to immunoblot analysis with the indicated antibodies. **(B)** Same as (A) but senescence was analyzed by histochemistry to determine the level of β-galactosidase activity measured at pH 6.0. Representative images of senescent cells are shown. **(C)** Same as (A) but examined for BrdU incorporation. Values represent the mean + SD. **(D)** Immunoblot analysis of human melanocytes from two healthy individuals (HM1-Mi^{WT}, HM2-Mi^{WT}) or from two different patients carrying the MITF^{E318K} mutation (HM1-Mi^{E318K}, HM2-Mi^{E318K}) who were transduced with control (EV) or BRAF^{V600E} lentiviral particles for 15 days. **(E)** Melanocytes were treated as described in (D) and stained for SA-βGal activity. Representative images of senescent cells are presented. **(F)** Quantification of SA-βGal staining.

Figure1

Click here to download Figure Bonet Fig1JNCI.jpg

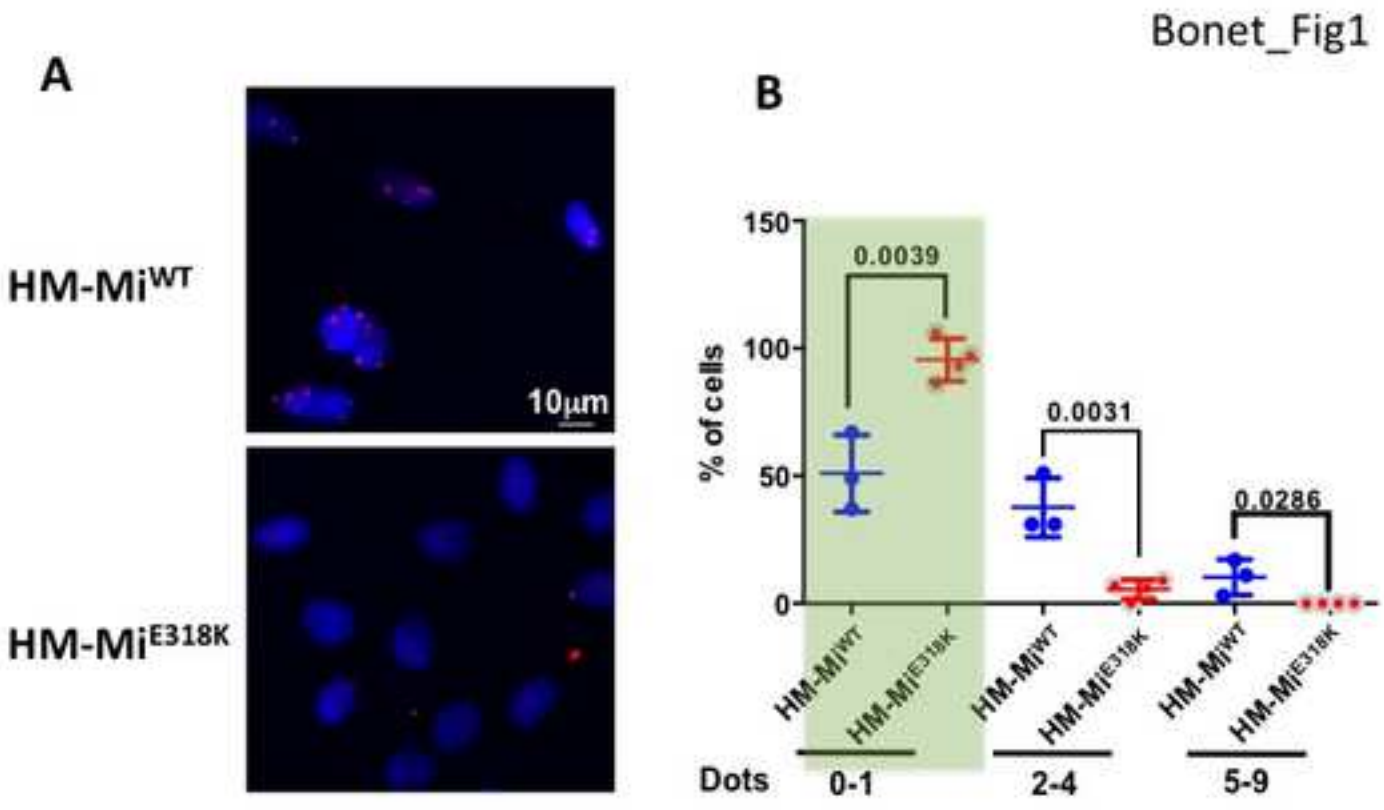

Figure2

Click here to download Figure Bonet Fig2JNCI.jpg

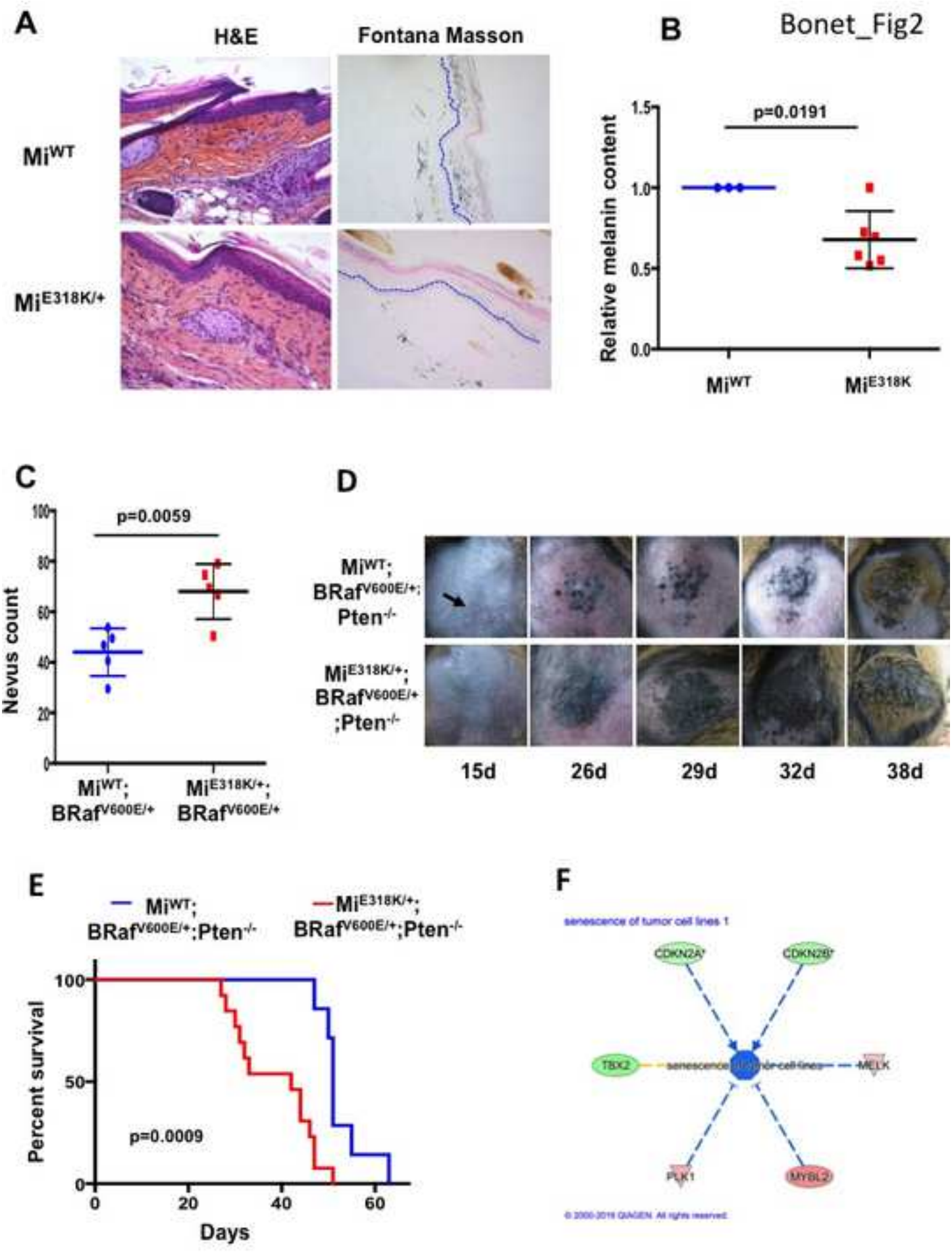

Figure3

Click here to download Figure BonetFIG3JNCI.jpg